JOURNAL OF PROPULSION AND POWER
Vol. 27, No. 2, March–April 2011

Technical Notes

Low-Order Model for Buzz Oscillations in the Intake of a Ramjet Engine

Ik-Soo Park,* N. Ananthkrishnan,† and Min-Jea Tahk‡
Korea Advanced Institute of Science and Technology, Daejeon 305-701, Republic of Korea
and
C. R. Vineeth§ and Nitin K. Gupta¶
IDeA Research and Development (P), Ltd., Pune 411013, India

DOI: 10.2514/1.50093

I. Introduction

BUZZ refers to the self-sustained oscillations of the terminal shock in a mixed-compression supersonic intake where it is periodically sucked into the intake duct and then forced out. Correspondingly, the air mass flow rate entering the intake and the intake backpressure (combustion chamber pressure) fluctuate. The related phenomenon where the terminal shock emerges and establishes itself outside the intake duct in a relatively steady manner is usually called unstart. Buzz oscillations have plagued every type of supersonic intake ever since the phenomenon was discovered by Oswatitsch [1], and ramjets are no exception [2,3]. There is a heightened risk of intake unstart or buzz for ramjet-powered vehicles during maneuvers such as accelerated climb where the fuel injection rate has to be delicately balanced between the increased thrust requirement and the decreasing air mass flow rate with altitude. Besides, atmospheric disturbances that may trigger buzz/unstart are the most severe at low altitudes, typical at the start of an accelerated climb segment [4,5]. Hence, there is a need to actively control the position of the terminal shock in the intake duct, usually by prescribing a certain unstart/buzz margin [6] or, equivalently, an intake backpressure (P4) margin [7]. The buzz or P4 margin is maintained by control action, usually by manipulating intake air bleed or by varying the exit nozzle throat area [8]. However, these measures are successful, provided the terminal shock is maintained inside the intake duct. Once unstart or full-fledged buzz has occurred, more severe control action is necessary, and a low-order model for large-amplitude buzz oscillations is required that is appropriate for controller design.

The flow mechanisms responsible for buzz have been known from the early work by Ferri and Nucci [9] and Dailey [10]. Many experimental [11,12] and computational studies [13–16] of the buzz phenomenon in supersonic intakes have been reported over the years. However, as commented by Trapier et al. [17], there have only been limited attempts to derive a theoretical model for buzz [18,19], and a good prediction for buzz onset is currently unavailable. Although the question of unstart/buzz onset may itself be addressed by linear models [20–22], full-fledged buzz is an unsteady, nonlinear phenomenon, with every buzz cycle passing through two distinct regimes of flow physics. In the supercritical regime, the terminal shock is inside the intake duct, and acoustic waves traveling back and forth between the intake and the combustion chamber can influence the shock position, and hence the intake total pressure recovery, while mass flow rate is largely unchanged [23]. In contrast, the shock is outside the intake duct in the subcritical regime, so the intake backpressure regulates the mass flow rate entering the duct while total pressure recovery is little affected. Obtaining a dynamical model for buzz has therefore been a challenge.

A low-order model for unstart dynamics and control, by considering the intake alone, has been derived by MacMartin [24]. For a coupled intake-combustor system, a low-order model for the supercritical regime has been developed in recent work by Gupta et al. [25], yielding a set of mathematical equations and relations [26] that could be successfully used for controller design [7]. In the spirit of this previous work, the present paper obtains a low-order dynamical model representing buzz oscillations in a ramjet engine with a variable-area nozzle throat. The buzz frequency is seen to be a function of a parameter B^*, similar to the B parameter in [25,26], and along the lines of the Greitzer [27] B parameter for compression systems.

II. Model Development

A typical ramjet engine layout with the different station numbers is sketched in Fig. 1. For the supercritical regime, a simplified version of the dynamical model in [25,26] is used by no longer solving explicitly for properties at station 5. The subcritical model has been obtained afresh. The models for both regimes have been compactly written in Table 1 and are described next.

Given the intake properties, the fuel injection rate $\dot{m}_f$, and the combustor pressure P_c (see the equation on line 5 of Table 1), a combustion model is used to obtain the other flow properties in the combustion chamber. The combustion model may be a quasi-1d model, as described in [25], or a simpler 0d model, as shown next, presently used in this work:

$$\dot{m}_{c_{ss}} = \dot{m}_4 + \dot{m}_f \tag{1}$$

$$T_{07_{ss}} = \frac{\dot{m}_4 T_{04} + (\dot{m}_f \eta_c Q)/C_p}{\dot{m}_4 + \dot{m}_f} \tag{2}$$

$$P_{07_{ss}} = r_c P_{04} \tag{3}$$

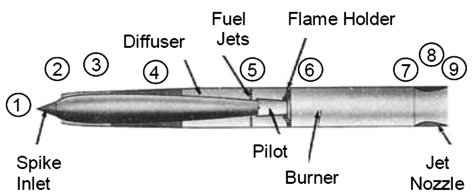

Fig. 1 Typical ramjet configuration with station numbers (1: nose cone, 2: cowl lip, 3: terminal shock, 4: backpressure sensor location, 5: fuel injection, 6: pilot flame, 7: combustor exit, 8: nozzle throat, and 9: nozzle exit).

Received 29 March 2010; revision received 10 November 2010; accepted for publication 12 November 2010.

*Ph.D. Student, Division of Aerospace Engineering, 373-1 Guseong-dong, Yuseong-gu; ispak@fdcl.kaist.ac.kr.
†Research Professor, Division of Aerospace Engineering, 373-1 Guseong-dong, Yuseong-gu; drakn19@kaist.ac.kr.
‡Professor, Division of Aerospace Engineering, 373-1 Guseong-dong, Yuseong-gu; mjtahk@fdcl.kaist.ac.kr.
§Associate, Magarpatta City, Hadapsar; vineeth@idearesearch.in.
¶CEO, Magarpatta City, Hadapsar; nitin@idearesearch.in.

Table 1 Dynamical model for supercritical and subcritical regimes

Line	Supercritical	Subcritical
1	$\dot{P}_c = (1/B^*)[\dot{m}_c - A_{\text{th}} r_n (P_{07}\beta/\sqrt{T_{07}})]$	$\dot{P}_c = (1/B^*)[\dot{m}_c - A_{\text{th}} r_n (P_{07}\beta/\sqrt{T_{07}})]$
2	$P_{4_{ss}} = P_c$	
3	$\dot{P}_4 = (1/\tau_u)(P_{4_{ss}} - P_4)$	$\ddot{m}_4 = (A_i/L_i)(P_4 - P_c)$
4	$P_4, \{1\} \longrightarrow \dot{m}_4, T_{04}, P_{04}$	$\dot{m}_4, \{1\} \longrightarrow P_4, T_{04}, P_{04}$
5	$\dot{m}_4, T_{04}, \dot{m}_f, P_c \longrightarrow \dot{m}_{c_{ss}}, T_{07_{ss}}, P_{07_{ss}}$	$\dot{m}_4, T_{04}, \dot{m}_f, P_c \longrightarrow \dot{m}_{c_{ss}}, T_{07_{ss}}, P_{07_{ss}}$
6	$\ddot{m}_c = (1/\tau_d)(\dot{m}_{c_{ss}} - \dot{m}_c)$	$\ddot{m}_c = (1/\tau_d)(\dot{m}_{c_{ss}} - \dot{m}_c)$
7	$\dot{T}_{07} = (1/\tau_d)(T_{07_{ss}} - T_{07})$	$\dot{T}_{07} = (1/\tau_d)(T_{07_{ss}} - T_{07})$
8	$\dot{P}_{07} = (1/\tau_d)(P_{07_{ss}} - P_{07})$	$\dot{P}_{07} = (1/\tau_d)(P_{07_{ss}} - P_{07})$

where r_c is the combustor loss coefficient, η_c is the combustor efficiency, Q is the fuel heating value, and C_p is the specific heat. These properties are updated based on a first-order delay model (see the equations on lines 6–8 of Table 1), where τ_d is the lag in the downstream direction that depends on the mean flow velocity. These relations are common to both of the regimes.

The nozzle properties are given by the isentropic relation:

$$T_{08} = T_{07} \quad \text{and} \quad P_{08} = r_n P_{07} \tag{4}$$

where r_n is the nozzle loss coefficient. Subsequently, the choking mass flow at the nozzle throat may be computed, and the difference between the mass flow in the combustion chamber and that exiting the nozzle yields the combustion chamber pressure, as indicated by the equation on line 1 of Table 1. Here, A_{th} is the nozzle throat area, and β and B^* are defined as [7,26]

$$\beta = \sqrt{\frac{\gamma_h}{R}}\left(\frac{2}{\gamma_h + 1}\right)^{(\gamma_h+1)/[2(\gamma_h-1)]}, \qquad B^* = \int_6^7 \frac{A_c}{\gamma R T(x)}\,\mathrm{d}x \tag{5}$$

where γ_h is the hot gas specific heat, A_c is the combustor cross-sectional area, and B^* is best obtained from a quasi-1d code [25]. This too is common to both the regimes.

Where the models for the two regimes differ is in the handling of the intake. For the supercritical case, the intake backpressure is dictated by the combustor pressure, and it may be obtained in the steady state from a quasi-1d code, as in [25], or more simply by the equation on line 2 of Table 1. In the transient, $P4$ is updated by a first-order lag model in the equation on line 3 of Table 1, representing the delay due to acoustic wave propagation upstream from the combustion chamber to the intake against the mean flow velocity, given by τ_u. As long as the terminal shock remains within the intake, this acoustic signal cannot travel further upstream to the cowl lip, and thus cannot influence the air mass flow rate entering the intake. Hence, given the backpressure $P4$ and the freestream conditions $\{1\}$, the properties at station 4 (Fig. 1) can be read from the intake relation equations on line 4 of Table 1, to be described next. On the other hand, for a subcritical intake, a change in combustor pressure P_c can be felt all the way to the cowl lip, and it affects the mass flow entering the intake duct. An increase in P_c will encourage spillage at the cowl lip, reducing the mass flow rate, whereas a decrease in P_c can draw more air mass flow into the intake, and with it perhaps also suck the shock back into the intake. Thus, for the subcritical case, there is no equivalent of the equation on line 2 of Table 1 for the supercritical intake, and the change in intake mass flow rate must be modeled as in the equation on line 3 of Table 1. Now, the intake mass flow rate along with the freestream conditions $\{1\}$ is used to read up the station 4 properties from the equation on line 4 of Table 1, exactly converse to the supercritical case. The equation on line 3 of Table 1 for the intake mass flow rate are similar to that in Greitzer [27] or Badmus et al. [28], where A_i and L_i refer to the effective intake cross-sectional area and length, respectively.

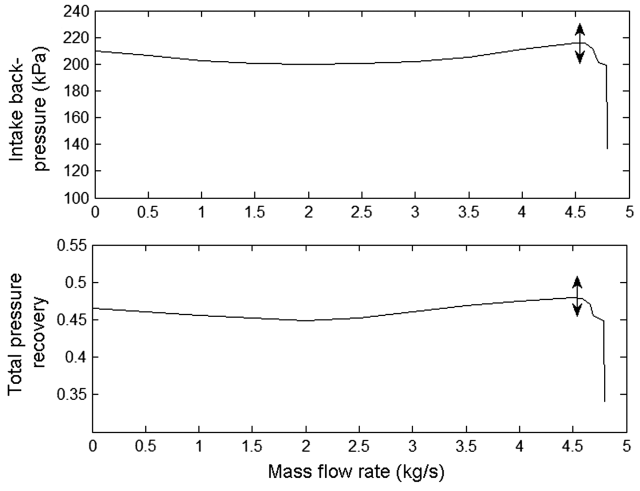

Fig. 2 Intake static pressure rise and total pressure recovery characteristic.

The intake relation in the equations on line 4 of Table 1 are usually specified in terms of a characteristic of static pressure rise and total pressure recovery as a function of mass flow rate. A typical intake characteristic, used in the present study, is shown in Fig. 2. Of this, the supercritical leg and a brief subcritical segment to the right of the arrow may be obtained from steady-state numerical computations, as described in [25,26]. The subcritical segment to the left of the arrow is really the unstable part of the characteristic, and its general shape is prescribed based on the description in [10,29]. Total temperature T_{04} may be taken to be the same as the freestream total temperature T_{01}. Applying the equations on line 4 of Table 1 to the intake characteristic for a given P_4 in the supercritical case and the given $\dot{m}_4$ in the subcritical case makes sense physically and from a numerical sensitivity point of view.

III. Simulation

The model developed here is used to simulate a buzz oscillation cycle for the ramjet configuration studied previously [25,26]. The main parameters of interest are listed in Table 2. Exit nozzle throat

Table 2 Ramjet system parameters for buzz simulation

Freestream	Intake	Combustor	Other	Nozzle
$M = 3.0$	$A_i = 0.026$ m^2	Fuel–air ratio $= 0.04$	$\tau_d = 0.007$	$r_n = 1$
$H = 10.0$ km	$L_i = 1.36$ m	$\eta_c = 0.99$	$\tau_u = 0.003$	$\gamma_h = 1.4$
Angle of attack $= 0$		$r_c = 0.95$	$C_p = 1000$ kg/K $\cdot$ s	A_{th} variable
		$Q = 45$ MJ/kg	$\gamma = 1.4$	
		$B^* = 3.10^{-7}$ m $\cdot$ s^2	$R = 287$ J/kg $\cdot$ K	
		$A_c = 0.061$ m^2		

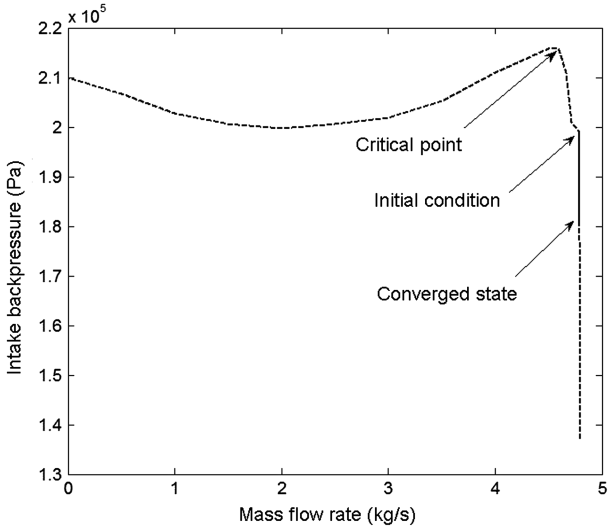

Fig. 3 Intake characteristic (dashed line) showing initial condition, critical point, and simulation (full line) converged to supercritical state for $A_{\text{th}} = 0.03$ m^2.

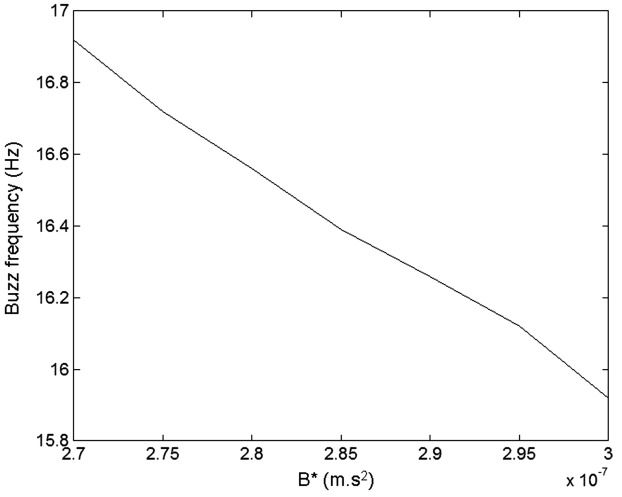

Fig. 5 Variation of buzz frequency with B^* parameter for fixed $A_{\text{th}} = 0.0254$ m^2.

area is the variable parameter. The initial condition for the simulations is selected as

$$\dot{m}_4 = 4.78 \text{ kg/s}, \qquad P_4 = 199 \text{ kPa}, \qquad \dot{m}_c = 4.97 \text{ kg/s}$$
$$T_{07} = 2309 \text{ K}, \qquad P_{07} = 206 \text{ kPa}$$

The model in Table 1 is a switched dynamical system with state-dependent switching. As the mass flow rate corresponding to the critical point (see Fig. 3) is crossed, the system is switched between subcritical and supercritical submodels. The state variables are passed from one submodel to the other, and the integration time is reset. An initial simulation is done for the throat area, $A_{\text{th}} = 0.03$ m^2. For a small perturbation to the initial condition shown previously, the system converges to a steady supercritical state, as shown in Fig. 3. Further simulations are carried out with decreasing values of A_{th} until the point of instability onset is identified as $A_{\text{th}} = 0.0255$ m^2. For a value slightly below this, such as $A_{\text{th}} = 0.0254$ m^2, a small perturbation (from the same initial condition) leads to a buildup of oscillations ending up in a full-fledged sustained buzz limit cycle. This is shown in the phase plane and in the mass flow rate, intake backpressure time histories in Fig. 4. The oscillations build up to constant amplitude and fixed frequency, typical of limit cycles. The mass flow rate time history shows a typical profile with a near-constant supercritical peak followed by a rapid excursion to a low subcritical valley and back. In the phase plane, as the oscillations develop, the system first goes along the subcritical characteristic before being repelled back to the supercritical segment. However, further cycles loop around the subcritical leg of the characteristic, indicating that it is indeed an unstable segment. The extent of travel of the terminal shock can be gauged from the leftmost point on the phase plane in Fig. 4, where the buzz cycle intersects the subcritical leg, and from the point at which the cycle reattaches to the supercritical leg.

From the time history plots in Fig. 4, the frequency of buzz oscillations can be estimated to be nearly 16 Hz. This is similar to typical buzz frequencies reported in the literature: for example, in [11,17]. Varying B^* over a range of 10% below its value in Table 2 reveals the effect of B^* on the buzz frequency, as shown in Fig. 5. As the parameter B^* is correlated with the combustion chamber volume, the buzz frequency is seen to fall with an increase in chamber volume. Interestingly, precisely the same effect is seen experimentally in compression systems for the surge frequency with increasing plenum chamber volume [30].

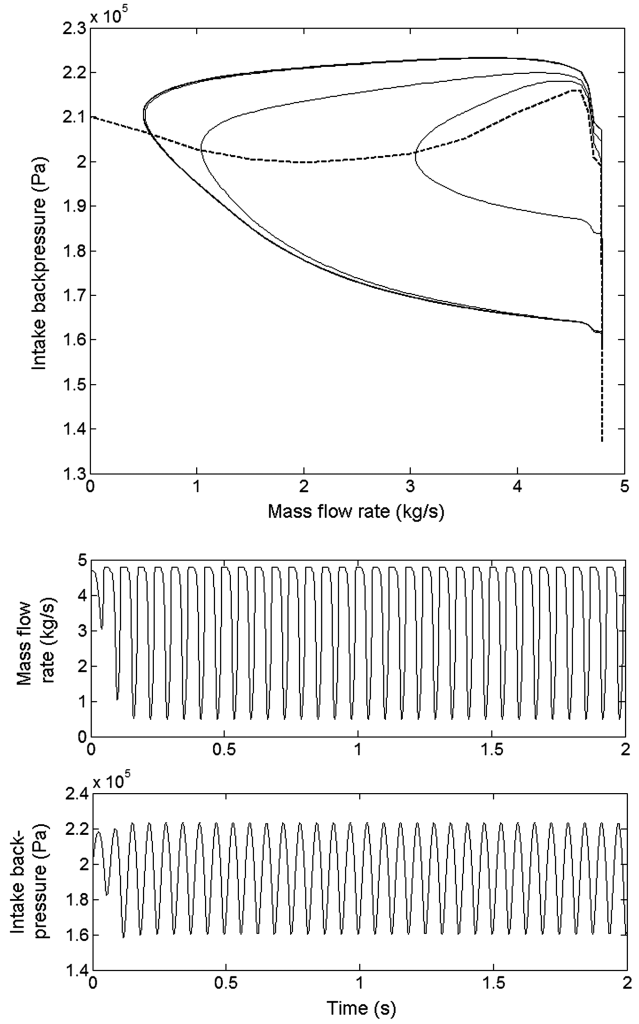

Fig. 4 Buzz limit cycles in phase plane and mass flow rate; intake backpressure time histories for $A_{\text{th}} = 0.0254$ m^2.

IV. Conclusions

A low-order dynamical model has been developed that captures the phenomenon of buzz oscillations in a supersonic intake. The model successfully couples the dynamics of the intake and the

subsonic combustor and the interaction between them, and it correctly represents the different physics of the intake in subcritical and supercritical operation. This yields a nonlinear, switched dynamical system that, when simulated for a typical ramjet engine configuration, shows limit cycle oscillations of a character and frequency similar to those observed in experiments in similar systems. The key parameters in the model are exit nozzle throat area A_{th} and B^*; A_{th} controls the onset of instability leading to the buzz cycle, and the buzz frequency is seen to be a function of B^*.

References

[1] Oswatitsch, K., "Pressure Recovery for Missiles with Reaction Propulsion at High Supersonic Speeds (The Efficiency of Shock Diffusers)," NACA TM 1140, 1947.

[2] Sterbentz, W., and Evvard, J., "Criterions for Prediction and Control of Ram-Jet Flow Pulsations," NACA RM E51C27, 1951.

[3] Trimpi, R., "A Theory for Stability and Buzz Pulsation Amplitude in Ram Jets and an Experimental Investigation Including Scale Effects," NACA Rept. 1265, 1956.

[4] Mayer, D. W., and Paynter, G. C., "Prediction of Supersonic Inlet Unstart Caused by Freestream Disturbances," *AIAA Journal*, Vol. 33, No. 2, 1995, pp. 266–275. doi:10.2514/3.12418

[5] Ahsun, U., Merchant, A., Paduano, J. D., and Drela, M., "Design of Near-Isentropic Supersonic Inlet Using Active Control," *Journal of Propulsion and Power*, Vol. 21, No. 2, 2005, pp. 292–299. doi:10.2514/1.7709

[6] Daren, Y., Tao, C., and Wen, B., "Equilibrium Manifold Linearization Model for Normal Shock Position Control Systems," *Journal of Aircraft*, Vol. 42, No. 5, Sept.–Oct. 2005, pp. 1344–1347. doi:10.2514/1.12845

[7] Chandra, K. P. B., Gupta, N. K., Ananthkrishnan, N., Park, I. S., and Yoon, H. G., "Modeling, Simulation, and Controller Design for an Air-Breathing Combustion System," *Journal of Propulsion and Power*, Vol. 26, No. 3, 2010, pp. 562–574. doi:10.2514/1.42368

[8] Boksenbaum, A. S., and Novik, D., "Control Requirements and Control Parameters for a Ram Jet with Variable-Area Exhaust Nozzle," NACA RM E8H24, Nov. 1948.

[9] Ferri, A., and Nucci, L. M., "The Origin of Aerodynamic Instability of Supersonic Inlets at Subcritical Conditions," NACA RM L50K30, 1951.

[10] Dailey, C. L., "Supersonic Diffuser Instability," Ph.D. Thesis, California Inst. of Technology, Pasadena, CA, 1954.

[11] Trapier, S., Duveau, P., and Deck, S., "Experimental Study of Supersonic Inlet Buzz," *AIAA Journal*, Vol. 44, No. 10, 2006, pp. 2354–2365. doi:10.2514/1.20451

[12] Hirschen, C., Herrmann, D., and Gülhan, A., "Experimental Investigations of the Performance and Unsteady Behavior of a Supersonic Intake," *Journal of Propulsion and Power*, Vol. 23, No. 3, 2007, pp. 566–574. doi:10.2514/1.25103

[13] Newsome, R., "Numerical Simulation of Near-Critical and Unsteady, Subcritical Inlet Flow," *AIAA Journal*, Vol. 22, No. 10, 1984, pp. 1375–1379. doi:10.2514/3.48577

[14] Lu, P.-J., and Jain, L.-T., "Numerical Investigation of Inlet Buzz Flow," *Journal of Propulsion and Power*, Vol. 14, No. 1, Jan.–Feb. 1998, pp. 90–100. doi:10.2514/2.5254

[15] Trapier, S., Deck, S., and Duveau, P., "Delayed Detached-Eddy Simulation and Analysis of Supersonic Inlet Buzz," *AIAA Journal*, Vol. 46, No. 1, 2008, pp. 118–131. doi:10.2514/1.32187

[16] Yeom, H.-W., Kim, S.-J., Sung, H.-G., and Yang, V., "Inlet Buzz and Combustion Oscillation in an Axisymmetric Ramjet Engine," 48th AIAA Aerospace Sciences Meeting, Orlando, FL, AIAA Paper 2010-756, 4–7 Jan. 2010.

[17] Trapier, S., Deck, S., Duveau, P., and Sagaut, P., "Time-Frequency Analysis and Detection of Supersonic Inlet Buzz," *AIAA Journal*, Vol. 45, No. 9, Sept. 2007, pp. 2273–2284. doi:10.2514/1.29196

[18] Willoh, R. G., "A Mathematics Analysis of Supersonic Inlet Dynamic," NASA TND-4969, Aug. 1968.

[19] Leynaert, J., "Pompage dans les Entrées d'Air Supersoniques," *L'Aéronautique et l'Astronautique*, Vol. 22, No. 6, 1970, pp. 47–62.

[20] Hurrell, H. G., "Analysis of Shock Motion in Ducts During Disturbances in Downstream Pressure," NACA TN 4090, Sept. 1957.

[21] Culick, F. E. C., and Rogers, T., "The Response of Normal Shocks in Diffusers," *AIAA Journal*, Vol. 21, No. 10, 1983, pp. 1382–1390. doi:10.2514/3.60147

[22] Moase, W. H., Brear, M. J., and Manzie, C., "The Forced Response of Choked Nozzles and Supersonic Diffusers," *Journal of Fluid Mechanics*, Vol. 585, 2007, pp. 281–304. doi:10.1017/S0022112007006647

[23] Oh, J. Y., Ma, F., Hsieh, S.-Y., and Yang, V., "Interactions Between Shock and Acoustic Waves in a Supersonic Inlet Diffuser," *Journal of Propulsion and Power*, Vol. 21, No. 3, May–June 2005, pp. 486–495. doi:10.2514/1.9671

[24] MacMartin, D., "Dynamics and Control of Shock Motion in a Near-Isentropic Inlet," *Journal of Aircraft*, Vol. 41, No. 4, July–Aug. 2004, pp. 846–853. doi:10.2514/1.416

[25] Gupta, N. K., Gupta, B. K., Ananthkrishnan, N., Shevare, G. R., Park, I. S., and Yoon, H. G., "Integrated Modeling and Simulation of an Airbreathing Combustion System Dynamics," AIAA Modeling and Simulation Technologies Conference and Exhibit, Hilton Head, SC, AIAA Paper 2007-6374, Aug. 2007.

[26] Ananthkrishnan, N., Walambe, R., Gupta, N. K., Choi, J. H., Park, I. S., and Yoon, H. G., "Novel Analytical Redundancy Relation for Intake Backpressure Sensor in an Airbreathing Engine," *Journal of Propulsion and Power*, submitted for publication.

[27] Greitzer, E. M., "Surge and Rotating Stall in Axial Flow Compressors, Part I: Theoretical Compression System Model," *Journal of Engineering for Power*, Vol. 98, No. 2, April 1976, pp. 190–198. doi:10.1115/1.3446138

[28] Badmus, O. O., Eveker, K. M., and Nett, C. N., "Control-Oriented High-Frequency Turbomachinery Modeling: General One-Dimensional Model Development," *Journal of Turbomachinery*, Vol. 117, No. 3, July 1995, pp. 320–335. doi:10.1115/1.2835666

[29] Connors, J. F., "Some Aspects of Supersonic Inlet Stability," NACA RM E55l16a, 1956.

[30] Rao, A. N. V., and Ramesh, O. N., "The Dynamics of Surge in Compression Systems," *Sadhana: Academy Proceedings in Engineering Sciences*, Vol. 32, Nos. 1–2, Feb.–April 2007, pp. 43–47. doi:10.1007/s12046-007-0004-z

C. Segal
Associate Editor